Interaction of NaI with Solid Water and Methanol

O. Höfft, U. Kahnert, S. Bahr, and V. Kempter*

Technische Universität Clausthal, Institut für Physik und Physikalische Technologien, Leibnizstr. 4, D-38678 Clausthal-Zellerfeld, Germany

Received: April 28, 2006; In Final Form: June 26, 2006

The interaction of NaI with amorphous solid water (ASW) and methanol (MeOH) has been investigated with metastable impact electron spectroscopy (MIES), UPS(HeI), and temperature programmed desorption (TPD). We have studied the electron emission from the ionization of the highest-lying states of H_2O, CH_3OH, and of 5pI. We have prepared NaI layers on ASW (MeOH) films at about 105 K and annealed them up to about 200 K. Surface segregation of iodide is observed in ASW, as predicted for NaI aqueous solutions.[1] On the other hand, surface segregation is not observed in MeOH, again as predicted for the interaction of NaI with liquid methanol.[2] Electronic properties (ionization potentials, optical band gaps) and water binding energies are reported and are analyzed on the basis of available DFT results for hydrated NaI clusters.[3]

1. Introduction

The understanding of the interaction of halide salt molecules with solvents, water in particular, is of interest in various fields, ranging from biological systems to catalysis and environmental sciences. Hydrated salt particles extracted from the ocean may become part of the atmosphere or deposited on the ocean shore. In both situations, they play an important role as providers for halide species and/or catalysts for pollution reactions.[4,5]

Molecular dynamics (MD) calculations have been performed on a number of solvated alkali halides (denoted by MX in the following) at the vacuum−solvent interface.[1,2,6] For water, it was concluded that, as the size of the halide ions increases, a spatial separation of cations and anions takes place in the interfacial region.[1]

A number of surface-analytical techniques have proven to be capable to provide detailed information on the saltwater interaction at low temperatures (below 140 K, typically): Low-energy sputtering (LES)[7] and reactive ion scattering (RIS)[8] have proven to be sensitive tools for monitoring surface-near species in saltwater systems. So far, nonlinear optical probes have only been applied to the surfaces of aqueous solutions of alkali halides.[9−11] Very recently, near-edge X-ray absorption fine structure (NEXAFS) spectra have been reported for solutions of NaCl in water[12] and NaI in water and ethanol.[13] In the metastable impact electron spectroscopy (MIES),[14,15] metastable He atoms of thermal energy interact via Auger processes exclusively with the species at the surface of the saltwater system. The ejected electrons bear information on the electronic structure of the surface top layer. In the past, we have applied the combination of the MIES and UPS with HeI to the study of the interaction of CsCl,[16,17] NaCl,[18] CsF,[19] and CsI[20] with amorphous solid water (ASW) and, in the case of CsI, also with MeOH. The spectroscopy results were backed-up by first-principles DFT[18] or classical MD calculations,[20] concentrating either on the electronic structure of solvated halide ions or on their solvation properties. We have presented evidence that solvation effects, similar to those found in water, do also occur when MX species interact with ASW.

The exact nature of ASW and its relation to liquid water and ice is a matter of active research. It has been speculated (see discussion in ref 20) that ASW may, under certain conditions, be considered as a form of supercooled water, in particular as far as solvation processes are concerned. It was recently pointed out that the analogy between ASW and liquid water may even go further.[21] It appears logical to ask whether the analogy between ASW and liquid water also comprises the solvation mechanism itself. In this respect, the theoretical approach, often made to describe the solvation process in liquids, consists of the computation of the structure and the electronic properties of certain model complexes, as in particular solvent-shared (or solvent-separated) ion pairs $M^+(H_2O)_n)X^-$ as well as of the fully hydrated components M^+ and X^- ($M^+(H_2O)_p$ and $X^-(H_2O)_q$).[3,12,13,22,23] Experimentally accessible parameters include the ionization potentials of these complexes as well as the energies for detaching water molecules from them. Both properties show solvation effects as were demonstrated for hydrated NaX (X =: F to I) complexes.[3,22]

We apply valence electron spectroscopies (MIES, UPS) and temperature programmed desorption (TPD) to obtain information on the details of the solvation process. The best studied systems from the theoretical point of view are aqueous solutions of NaX species. On one hand, the segregation of X has been studied by classical MD.[1,9] On the other hand, a detailed cluster DFT study exists for $NaX(H_2O)_n$) (n = 1 to 6) clusters from which the desorption energetics as well as the IPs of the hydrated complexes can be obtained.[3] We present TPD and combined MIES and UPS(HeI) results for the interaction of NaI with ASW and MeOH surfaces, prepared at about 100 K and annealed until the solvents have desorbed completely (above 170 K, typically). The choice of solvents is suggested from our previous finding for CsI[20] that surface segregation of I^- takes place for ASW but not for MeOH.

2. Experimental Section

The apparatus, applied to the study of the salt−ASW and salt−MeOH interactions, has been described in detail previously.[16−18] A cold-cathode gas discharge source produces metastable He* atoms with about 20 eV of potential energy,

* To whom correspondence should be addressed. Tel: +49-5323-72-2363. Fax: -72-3600. E-mail: volker.kempter@tu-clausthal.de.

10.1021/jp0626014 CCC: $33.50
Published on Web 08/04/2006

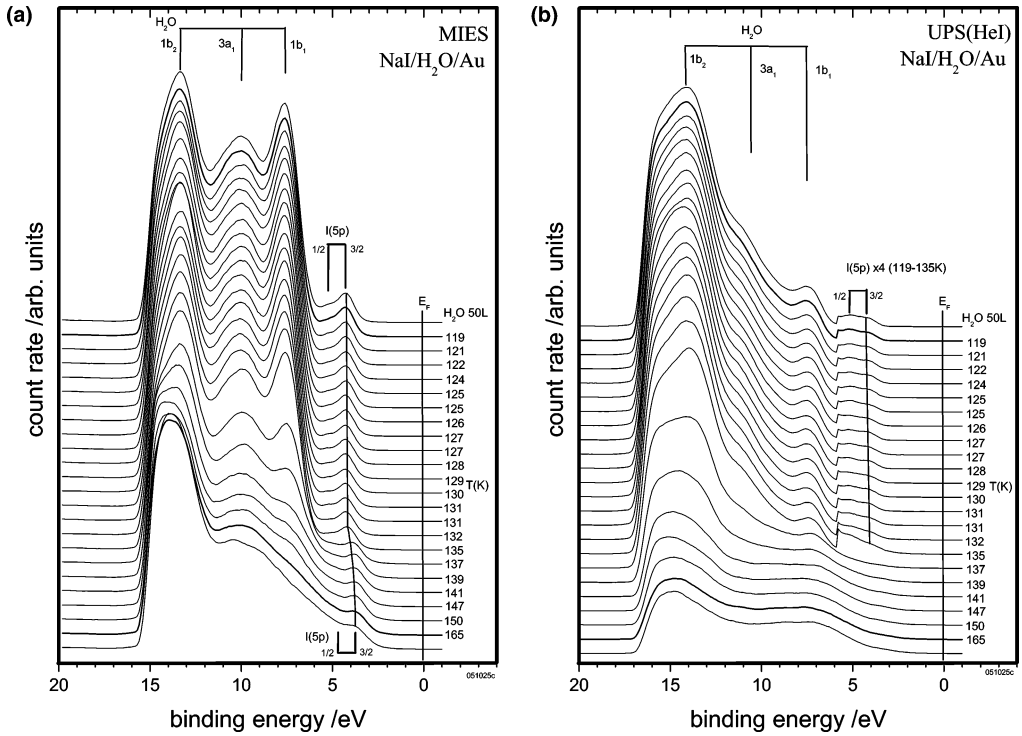

Figure 1. MIES (a) and UPS (HeI) (b) spectra for 0.5 ML NaI, deposited on amorphous solid water (ASW) at 105 K (top spectrum), and spectral changes recorded during annealing to 165 K. Acronyms as explained in the text.

but only thermal kinetic energy (60−100 meV) (for MIES), and HeI photons (21.2 eV) (for UPS). MIES is nondestructive and highly surface sensitive (see refs 14 and 15 for more detailed introductions into MIES and its various applications in molecular and surface spectroscopy). The spectral contributions from metastables and photons are separated by means of a time-of-flight technique. Electrons emitted by He* atoms and UV photons are analyzed in the direction normal to the surface using a hemispherical analyzer. By applying suitable biasing, electrons emitted from the Fermi level, E_F (as determined from the UPS spectra from the clean polycrystalline Au substrate), are registered at 19.8 eV (the potential energy of He*(2^3S)). With this choice, the onset of the spectra at low kinetic (high binding) energies occurs at the work function (WF) of the Au sample, and its variation with exposure directly gives the exposure dependence of WF. When annealing the prepared films, their temperature is ramped slowly (1 K/min). The time required to collect a pair of MIES and UPS spectra quasi-simultaneously is about 60 s.

The TPD experiments are carried out using a differentially pumped quadrupole mass spectrometer (QMS), connected to the UHV apparatus employed for the MIES/UPS studies. To obtain TPD spectra exclusively from the relevant surface area, the QMS is surrounded by a stainless steel housing with a 3 mm opening.[24] The ramping time in TPD is considerably shorter (1 K/s) than that in MIES and UPS (1 K/min). For this reason, the maximum desorption rate in MIES/UPS occurs about 15 K earlier than in TPD.

The Au sample is cooled with liquid nitrogen to 105 K and exposed to water or methanol by backfilling the chamber. The exposures are stated in Langmuirs (L) (1 L = 10^{-6} Torr·s). It is expected that ASW is formed during the slow deposition of water vapor at temperatures below 120 K (see also the discussion in ref 20). On the basis of previous MIES results, we estimate that 4 L correspond to about 1 monolayer (ML) of water, in the sense that at this stage no substrate emission can be seen with MIES. By varying the film thickness, we have verified that there is no influence of the substrate onto the reported results at the film thicknesses typically applied in this work (12 ML). NaI was deposited by evaporating polycrystalline salt at about 700 K. Our previous results for salt adsorption on metals (tungsten) indicate a WF decrease until a surface coverage of 0.5 ML is reached.

3. Results and Interpretation

All results are presented as function of the binding energy, E_B, of the emitted electrons with respect to the Fermi level. As in refs 18, 19, and 20, we suppose that the intensity of the spectral features recorded with MIES directly reflects the density of states at the surface of the system under study.

The spectral features recorded for NaI−ASW were identified in refs 19 and 20 and are denoted by $1b_1$, $3a_1$, and $1b_2$ (emission from the three weakest-bound MOs of H_2O) and I(5p) (emission from the $5p_{1/2;3/2}$I states, displaying a fine structure splitting of about 1 eV). The MeOH-induced features, denoted by M_{1-5}, were identified in refs 20 and 25. By adding the WF to the reported E_B values, the vertical ionization potentials (IPs) of the states involved in the ionization process are obtained.

The TPD spectra are collected at a linear heating rate of 1 K/s, and routinely, five different masses are measured simultaneously.

3.1. Electron Energy Spectra. 3.1.1. Interaction of NaI with ASW. The top spectra of parts a and b of Figure 1 are for 0.5 ML NaI deposited on a H_2O film (about 12 BL thick) at 105 K. Besides the I(5p) feature, they display the structures from the ionization of the highest-lying MOs $1b_1$, $3a_1$, and $1b_2$ of H_2O. Both MIES and UPS (see blown-up section between 0 and about 6.5 eV) feature a partially resolved 5pI fine structure splitting of 1 eV. No contribution of secondary electrons to the emission denoted by $1b_2$ H_2O can be noticed in MIES whereas in UPS secondary electrons may be responsible for the emission seen at the left side of the $1b_2$ structure. As all energies refer to the Fermi level, the vertical IPs with respect to the vacuum are

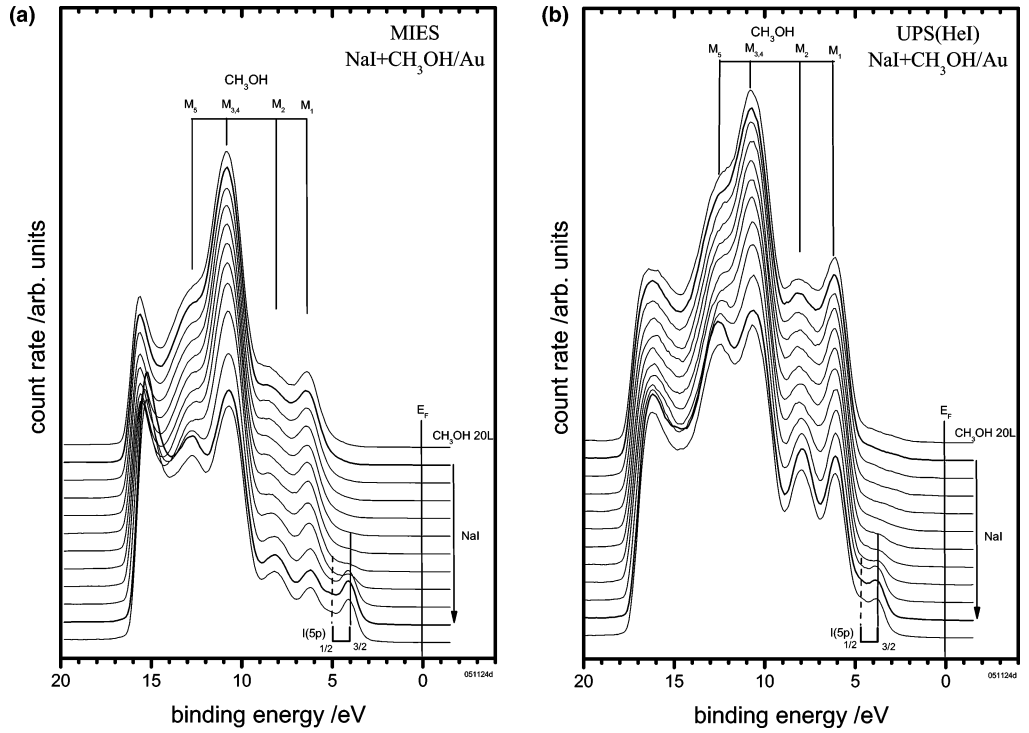

Figure 2. MIES (a) and UPS (HeI) (b) spectra during the deposition of 1 ML NaI onto polycrystalline Au, precovered by 20 L of methanol at 105 K (top), as a function of NaI exposure. Acronyms as explained in the text.

obtained by adding the WF (4.8 eV for the top spectrum in Figure 1a), as derived from the high-binding-energy cutoff of the spectrum. For neat water, we measure 10.2 eV for the distance between the valence band maximum and the vacuum level, close to the values reported for bulk water.[26] We determine 8.3 eV for the vertical IP of $5p_{3/2}$I in NaI on ASW to be compared with 7.7 eV for iodide in aqueous solution.[27]

Annealing of the NaI/ASW film leads to a decrease of the I(5p) intensity whereby the intensity minimum occurs around 132 K. It is correlated with the onset of the intensity decrease of the water features, signaling water desorption. Besides an increase of I(5p), we notice a decrease of the 5pI binding energy by about 0.5 eV and, because the WF remains unchanged, also a corresponding decrease of the vertical IP. As for CsI/ASW, I(5p) remains visible throughout the entire annealing procedure, although the intensity passes a minimum during the annealing procedure. This is at variance with NaI/MeOH: as will be shown below, I(5p) does indeed disappear almost completely during annealing. The same behavior has been noticed for CsI/ASW and MeOH.[20] In ref 20, we have attributed this behavior to the segregation of iodide at the ASW, but not at the solid MeOH surface. Surface segregation of heavy halide ions in liquid water, but not in liquid MeOH, has been predicted by classical MD calculations[1,2] performed for NaI aqueous and MeOH solutions and is the subject of two recent reviews.[9,28]

The portion of the total surface area occupied by iodide species (surface area accessed (ASA) by iodide[20]) is accessible by both theory and experiment. To obtain information on the ASA from the present MIES results, we proceeded as in ref 20: we monitored the decrease of the $1b_1$ H_2O signal (exposure 50 L, thickness about 10 ML) during the NaI deposition (0.5 ML), followed by heating of the sample up to 125 K, a temperature high enough to guarantee that the ionic species Na^+ and I^- can enter the ASW film. By an appropriate choice of the temperature ramp, we made sure that thermodynamic equilibrium is present during the annealing procedure on the time scale of the experiment. We can then estimate that the ASA of iodide is roughly 20%. Theory predicts a similar ASA value for a 1 M aqueous solution of CsI.[20]

3.1.2. Interaction of NaI with MeOH. We have separated the NaI/MeOH results into two parts, the deposition of NaI at about 105 K onto the MeOH film under "in situ" control of MIES and UPS (Figure 2 for 1 ML NaI) and the annealing of the NaI adlayer on MeOH up to about 185 K, again under MIES and UPS control (Figure 3 for 0.5 ML NaI). The 5pI fine structure splitting is largely masked by the strong MeOH emission (M_1). The MeOH film shows the structures M_{1-5} whereby M_2 and M_5 do, other than in the gas phase, not appear as well-developed peaks (in contrast to M_1 and $M_{3,4}$, both of which appear better defined). As a consequence of the NaI deposition onto the MeOH film, manifested by the appearance of the structure I(5p), M_2 and M_5 sharpen considerably. We offer the following explanation for the observed MeOH-induced peak sharpening: we consider M_2 and M_5 as network-forming MOs, inspired by the fact that they are directed within the plane of the MeOH network. On the other hand, M_1 and $M_{3,4}$ are π-type MOs in the sense that they are directed perpendicular to the network and, thus, are not involved in network formation. Apparently, the NaI deposition destroys the MeOH network in the near-surface region. As a consequence, the bonding MOs, being not involved in the network formation anymore, sharpen considerably, that is, M_2 and M_5 turn into well-defined, gas-phase-like peaks. As was already recognized in ref 20, the structure $M_{3,4}$, relative to the rest of the MeOH-induced emission, is much more pronounced in MIES than in UPS; this was attributed to the fact that the methyl group of MeOH is directed away from the film surface and, consequently, is efficiently accessed by the He* probe atoms employed in MIES. As described in section 3.1.1, we obtain the distance between the valence band maximum and the vacuum level (8.9 eV); the vertical IP of 5pI in NaI/MeOH amounts to 8.3 eV. The emission noticed in MIES for binding energies >13.5 eV is due to secondary electrons. The WF of NaI/MeOH is 4 eV, decreasing to about 3.5 eV during annealing.

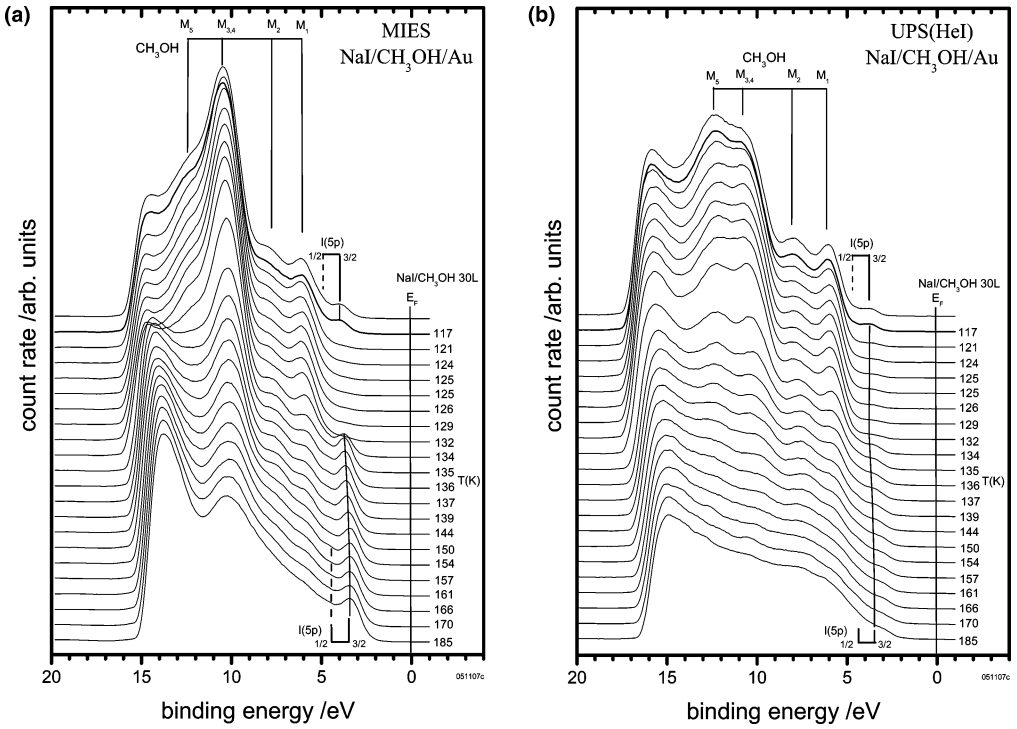

Figure 3. MIES (a) and UPS(HeI) (b) spectra of 0.5 ML NaI, deposited on a methanol film at 105 K (top), and spectral changes recorded during annealing to 185 K.

Annealing of 0.5 ML NaI on MeOH (Figure 3) leads to an almost complete disappearance of the I(5p) intensity prior to MeOH desorption. This indicates that NaI becomes almost completely solvated before MeOH desorption sets in, in contrast to ASW where surface iodide is at most partially solvated. The minimum is correlated with an intensity decrease of the MeOH features, caused by the beginning water desorption. The renewed increase of I(5p) intensity is accompanied by a decrease of the 5pI binding energy (0.2 eV) and, because the WF remains unchanged, also by a corresponding decrease of the vertical IP. This decrease is however smaller than that observed for ASW (0.5 eV). Although desorption starts already around 126 K, MeOH features remain visible up to at least 165 K (see also the discussion of the TPD spectra). In contrast to ASW, there are no indications for surface activity of NaI on MeOH; the same situation was noticed for the interaction of CsI with ASW and MeOH.[20]

3.2. Temperature Programmed Desorption Spectra (TPD). Figure 4 displays the TPD spectra recorded on mass 18 (H_2O) for neat water (20 L) on Au (a), as well as for 0.7 ML NaI deposited on ASW films of various thicknesses. Figure 5 presents analogous data for the interaction of NaI with MeOH. The desorption of the neat "solvents", ASW (MeOH), produces narrow structures around 158 (132 K) which we attribute to multilayer desorption. Initially, these peaks develop a tail toward higher temperatures as the consequence of the NaI deposition. When decreasing the H_2O (MeOH) film thickness while keeping the amount of NaI deposited constant, the narrow structures from the neat "solvents" are gradually replaced by broad structures, exhibiting some fine structure (NaI/MeOH). Their onset on the low-temperature side still essentially coincides with the onset of desorption from the neat "solvents" water (MeOH). On the other hand, it extends to about 220 (260) K for ASW (MeOH). This signals that the NaI−solvent interaction gives rise to a broad range of H_2O (MeOH) binding energies, extending from about 42 (34) kJ·mol^{-1} (close to the values for desorption from the neat multilayers) to more than 60 kJ·mol^{-1} for the strongest-

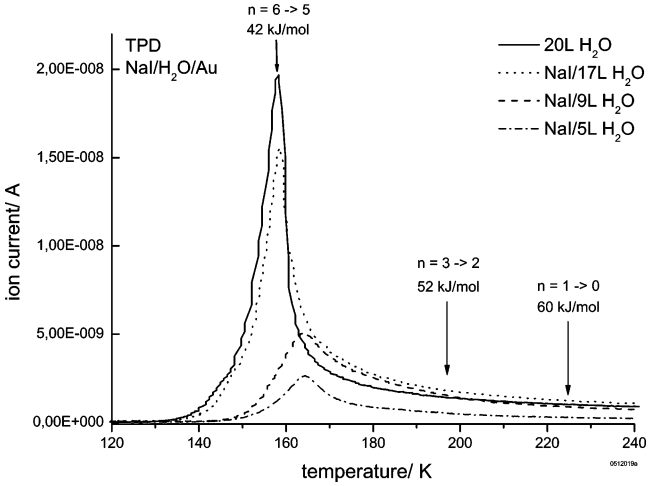

Figure 4. TPD spectra on mass 18 (H_2O) recorded for desorption of neat water and for NaI (0.7 ML) interacting with ASW films of various thicknesses.

bound species. The arrows displayed in Figure 4 indicate the temperature of the maximum desorption rate for the indicated desorption energies, calculated under the assumption of first-order desorption.[29] The corresponding analysis is presented for MeOH in Figure 5.

3.3. Binding Energies and Electronic Properties. Recently, cluster DFT computations were performed on $NaX(H_2O)_n$ structures (X =: F through I and $n = 1-6$) with the intention to compute the electronic and IR spectroscopy properties of aqueous halide solutions.[3,22,30] In accordance with earlier work on NaCl, at least five H_2O molecules appear to be required to dissociate NaX to be under the influence of the interacting H_2O molecules.[31]

In the following, we analyze our TPD and MIES/UPS results, for NaI interacting with ASW, on the basis of the above-mentioned computations. Where appropriate, we try to extend our conclusions also to MeOH. Both for ASW and MeOH, the

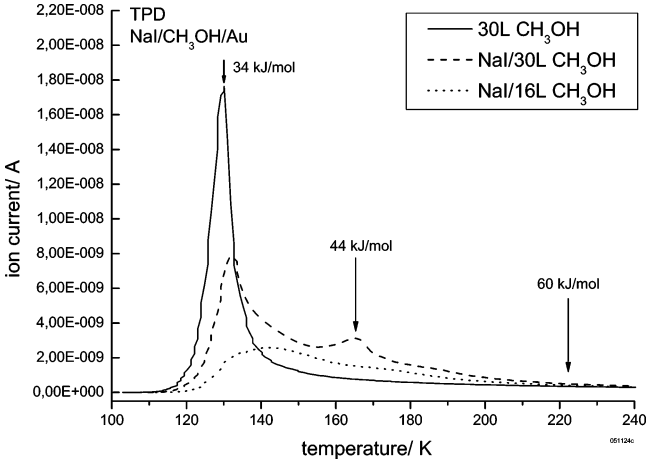

Figure 5. TPD spectra on mass 31 (CH_3OH) recorded for desorption of neat methanol and for NaI (0.7 ML) interacting with solid methanol films of various thicknesses.

TPD peak shows a remarkable broadening toward higher temperatures under the influence of the supplied NaI molecules. This finding can be understood when adopting the following scenario: the preparation procedure forms hydrated NaI structures, eventually partially or fully dissociated in the sense of ref 3. When annealing, temperature increase first removes the weakest-bound water molecules, that is, those not involved in the hydration of NaI species. This is followed by the removal of H_2O molecules from the largest hydrated structures present in the solution; further increase of the temperature leads to the removal of water molecules from increasingly smaller structures. This process can be visualized as the transition from $NaX(H_2O)_n$ to $NaX(H_2O)_{n-1}$ whereby n decreases with increasing temperature; the required energies can be obtained from the inspection of Table 2 of ref 3. Accordingly, the energy required to remove water from comparatively large clusters ($n = 5$ and 6) is rather similar to that for removal from bulk water because for $n > 4$ the water−water interaction starts to dominate. Temperature increase detaches further H_2O molecules, that is, the transition from $(n - 1)$ to $(n - 2)$, and so forth, leads to increasingly stronger bound smaller hydrated structures. A comparatively steep increase can be noticed for $n = 3 \rightarrow 2$. This increase of the H_2O binding energy stems from the fact that below $n = 4$ all water molecules are in direct contact with the Na−I complex.[3] We have indicated in Figure 4 at which temperatures, according to ref 3, transitions from n to $(n - 1)$ take place for $n = 6$, 3, and 1. The picture that emerges is that the tail of the TPD peak, seen in Figure 4, originates from H_2O molecules that are involved in the solvation of NaI complexes. The low-temperature part of the tail is caused by comparatively weakly bound water molecules (cluster size $n > 3$); on the high-temperature side, the tail extends up to the temperature that is required for the transition $n = 1 \rightarrow 0$, that is, required to remove the last H_2O molecule from the NaI species. No computations of the properties of NaI−MeOH structures are presently available, but on the basis of our results, we expect the sketched scenario to also be valid for that case. The structure as seen around 195 K for NaI/MeOH may be due to the fact that the binding energies change abruptly when going from $n = 4 \rightarrow 3$.

Frequently, the IPs of MX species in interaction with, in particular, liquid water are analyzed under the assumption that MX is fully dissociated and the resulting species M^+ and X^- are solvated independently.[27] However, in the near-surface region, full separation of the M and X species should not be anticipated "a priori".[3,22] To discuss the observed solvation shift of I(5p), that is, the decrease of the 5pI IP during the annealing process, we rely on the electronic properties of $NaI(H_2O)_n$ ($n = 1$ to 6) clusters as computed by ref 3; the IPs of selected conformers with $n = 0-6$ are presented in their Table 6. The vertical IPs increase from 7.88 eV for unsolvated NaI to values between 8.3 and 8.61 eV for various $n = 6$ conformers. The IPs increase essentially up to $n = 3$ and only weakly thereafter. The same behavior has been found for hydrated NaCl structures.[22] To relate these results to our observations, we adopt the same model as for the analysis of the TPD spectra, namely, that the hydration effects seen during the annealing process are caused by successively detaching H_2O molecules from the structures. Following ref 3, near saturation of the coordination numbers of both Na and X is reached for $n = 3$: up to $n = 3$ water molecules coordinate both ions while for $n > 4$ a water−water interaction develops. We suggest that the solvation shift of IP takes place when the coordination still changes, that is, for $n < 4$ while for larger n the IP will change comparatively little.

Results available in the literature indicate that for MeOH and aqueous solutions the solvent molecules interact in a similar manner with halide (X^-) ions,[32,33] that is, the (X−H) and (X−O) distances as well as the (O−H) orientation with respect to the (X^-−O) axis are rather similar. Nevertheless, the presence of the methyl group in MeOH may, for steric reasons, reduce the solvation number for the MeOH as compared with the aqueous solution as it was found with neutron diffraction for Cl^- solvation in MeOH as compared with water.[32] This, in turn, will reduce the stabilizing action of the solvation shell in the MeOH case and will, therefore, explain the smaller solvation shift seen for NaI/MeOH.

Besides the IPs, already presented in section 3.1, the width of the (optical or vertical) (HOMO−LUMO) band gap, denoted as BG in the following, can in principle be obtained from the high-kinetic-energy cutoff, E_{kin}^{max}, of the emission caused by electron−electron scattering[34,35]

$$E_{kin}^{max} = E^* - 2BG + V_0$$

E^* is the excitation energy (19.8 (21.2) eV in MIES (UPS), respectively) and V_0 the distance from the LUMO to the vacuum level (electron affinity). V_0 and BG are related via

$$IP = BG - V_0$$

In the following, we anticipate that the overwhelming majority of the low-energy scattered electrons involves solvent molecules; in this case, IP is the distance from the valence band maximum to the vacuum. As mentioned in section 3.1.1, there is no indication for NaI/ASW of a contribution from scattered electrons to the MIES spectra. Consequently, by inserting E_{kin}^{max} equal to zero in the formula given above, we can only arrive at a lower bound for the optical band gap in neat ASW (9.6 eV). This is close to the value for bulk water reported by theory (10.4 eV).[26]

For neat MeOH, we find $E_{kin}^{max} = 1.8$ eV from Figure 3a and determine from the above formula an optical band gap of 9.1 (±0.2) eV for MeOH, that is, within the accuracy of the experiment the position of the vacuum level (8.9 eV above the top of the valence band) coincides with the LUMO and $|V_0|$ for MeOH is of the order of 0.2 eV.

4. Concluding Remarks

The interaction of NaI with amorphous solid water (ASW) and methanol (MeOH) has been investigated with metastable

impact electron spectroscopy (MIES), UPS (HeI), and temperature programmed desorption (TPD). Surface segregation of iodide is observed in ASW, as predicted for aqueous solutions of NaI.[1] On the other hand, this is not observed in MeOH, again as predicted for the interaction of NaI with liquid methanol.[2] In both cases, there is no indication for surface activity of the Na species.

The energetic distance from the top of the valence band to the vacuum is 10.2 (8.9) eV for ASW (MeOH), respectively. For NaI−ASW, the ionization potential of the 5pI-derived states of the solvated iodide species is compared with the predictions of recent cluster DFT computations for solvent-sharing, partially and fully dissociated NaI−H_2O structures.[3] The observed solvation shift of the 5pI ionization energy of about 0.5 eV agrees well with the predicted increase of the vertical ionization potential when going from unsolvated NaI to hexahydrated NaI species. Estimates for the (HOMO−LUMO) band gaps for ASW and solid MeOH are presented. The TPD spectra for NaI−water are analyzed on the basis of the results of ref 3. In particular, the shape and width of the TPD spectra can be understood as the successive detachment of H_2O molecules from NaI−water clusters. We suggest that the conclusions concerning the solvation effects on the IPs and the desorption energies, interpreted for NaI−water on the basis of the theory results of ref 3, do apply for NaI−MeOH as well. However, changes in details can be anticipated because full coordination of the ions is not reached at $n = 3$ (as for water), given the fact that MeOH, other than H_2O, cannot be expected to coordinate both ions at the same time, and for this reason, more MeOH molecules are required for the saturation of the coordination.

Our results present evidence that the electronic properties and the binding energies in the NaI−ASW system can be well accessed from cluster DFT calculations. We arrived at the same conclusion during our study of the Na−ASW interaction that leads to 3sNa solvation, followed by Na^+OH^- and H_2 formation.[36] In the present case, the electronic properties of the NaI−ASW (MeOH) systems can be reasonably well understood on the basis of DFT cluster calculations provided that the interionic interactions in solvent-sharing ion pairs are taken into account.

Acknowledgment. Discussions of various theory aspects of this work with P. Jungwirth (Prague), H. Kang (Seoul National University), and K. Kim (Pohang University) are acknowledged.

References and Notes

(1) Jungwirth, P.; Tobias, D. J. *J. Phys. Chem. B* **2002**, *106*, 6361.
(2) Dang, L. X. *J. Phys. Chem. A* **2004**, *108*, 9014.
(3) Olleta, A. C.; Lee, H. M.; Kim, K. S. *J. Chem. Phys.* **2006**, *124*, 024321.
(4) Ravishankara, A. *Science* **1997**, *276*, 1058.
(5) Gard, E.; et al. *Science* **1998**, *279*, 1184.
(6) Dietter, J.; Morgner, H. *Chem. Phys.* **1997**, *220*, 261.
(7) Kim, J. H.; Shin, T.; Jung, K. H.; Kang, H. *ChemPhysChem* **2005**, *6*, 1.
(8) Park, S.-C.; Pradeep, T.; Kang, H. *J. Chem. Phys.* **2000**, *113*, 9373.
(9) Jungwirth, P.; Tobias, D. J. *Chem. Rev.* **2006**, *106*, 1259.
(10) Gopalakrishnan, S.; Liu, D.; Allen, H. C.; Kuo, M.; Shultz, M. J. *Chem. Rev.* **2006**, *106*, 1155.
(11) Petersen, P. B.; Saykally, R. J. *Annu. Rev. Phys. Chem.* **2006**, *57*, 333.
(12) Aziz, E. F.; Zimina, A.; Freiwald, M.; Eisebitt, S.; Eberhardt, W. *J. Chem. Phys.* **2006**, *124*, 114502.
(13) Aziz, E. F.; Freiwald, M.; Eisebitt, S.; Eberhardt, W. *Phys. Rev. B* **2006**, *73*, 075120.
(14) Morgner, H. *Adv. At. Mol. Opt. Phys.* **2000**, *42*, 387.
(15) Harada, Y.; Masuda, S.; Osaki, H. *Chem. Rev.* **1997**, *97*, 1897.
(16) Borodin, A.; Höfft, O.; Krischok, S.; Kempter, V. *Nucl. Instrum. Methods Phys. Res., Sect. B* **2003**, *203*, 205.
(17) Borodin, A.; Höfft, O.; Krischok, S.; Kempter, V. *J. Phys. Chem. B* **2003**, *107*, 9357.
(18) Borodin, A.; Höfft, O.; Kahnert, U.; Kempter, V.; Poddey, A.; Blöchl, P. *J. Chem. Phys.* **2004**, *121*, 9671.
(19) Borodin, A.; Höfft, O.; Kempter, V. *J. Phys. Chem. B* **2005**, *109*, 16017.
(20) Höfft, O.; Borodin, A.; Kahnert, U.; Kempter, V.; Dang, L. X.; Jungwirth, P. *J. Phys. Chem. B* **2006**, *110*, 11971.
(21) Kang, H. *Acc. Chem. Res.* **2005**, *38*, 893.
(22) Godinho, S. S. M. C.; Cabral do Couto, P.; Costa Cabral, B. J. *J. Chem. Phys.* **2005**, *122*, 044316.
(23) Singh, N. J.; Yi, H. B.; Min, S. K.; Park, M.; Kim, K. S. *J. Phys. Chem. B* **2006**, *110*, 3808.
(24) Bahr, S.; Borodin, A.; Höfft, O.; Kempter, V.; Allouche, A. *J. Chem. Phys.* **2005**, *122*, 234704.
(25) Günster, J.; Krischok, S.; Kempter, V.; Stultz, J.; Goodman, D. W. *Surf. Rev. Lett.* **2002**, *9*, 1511.
(26) Cabral do Couto, P.; Estacio, S. G.; Costa Cabral, B. J. *J. Chem. Phys.* **2005**, *123*, 054510.
(27) Winter, B.; Weber, R.; Hertel, I. V.; Jungwirth, M. F. P.; Brown, E. C.; Bradforth, S. E. *J. Am. Chem. Soc.* **2005**, *127*, 7203.
(28) Chang, T. M.; Dang, L. X. *Chem. Rev.* **2006** *106*, 1305.
(29) Redhead, P. *Vacuum* **1962**, *12*, 203.
(30) Lee, H. M.; Kim, D.; Kim, K. S. *J. Chem. Phys.* **2002**, *116*, 5509.
(31) Jungwirth, P. *J. Phys. Chem. A* **2000**, *104*, 145.
(32) Yamagami, M.; Wakita, H.; Yamaguchi, T. *J. Chem. Phys.* **1995**, *103*, 8174.
(33) Hawlicka, E.; Swiatla-Wojcik, D. *J. Phys. Chem. A* **2001**, *106*, 1336.
(34) Munakata, T.; Hirooka, T.; Kuchitsu, K. *J. Electron Spectrosc. Relat. Phenom.* **1980**, *18*, 51.
(35) Günster, J.; Brause, M.; Mayer, T.; Hitzke, A.; Kempter, V. *Nucl. Instrum. Methods Phys. Res.* **1995**, *100*, 411.
(36) Ferro, Y.; Allouche, A.; Kempter, V. *J. Chem. Phys.* **2004**, *120*, 8683.